THE JOURNAL OF BIOLOGICAL CHEMISTRY VOL. 288, NO. 18, pp. 13046–13056, May 3, 2013

Discs Large 1 (Dlg1) Scaffolding Protein Participates with Clathrin and Adaptator Protein Complex 1 (AP-1) in Forming Weibel-Palade Bodies of Endothelial Cells[S]

Received for publication, November 30, 2012, and in revised form, March 25, 2013 Published, JBC Papers in Press, March 26, 2013, DOI 10.1074/jbc.M112.441261

Monique Philippe[‡], Thibaut Léger[§], Raphaëlle Desvaux[¶], and Laurence Walch[‡1]

From the [‡]INSERM U698, Université Paris 7, Hemostasis, Bio-Engineering and Cardiovascular Remodeling, CHU X. Bichat, 75018 Paris, France, the [§]Plateforme de Protéomique Structurale et Fonctionnelle, Institut Jacques Monod, UMR7592, Université Paris-Diderot, CNRS, 75013 Paris, France, and the [¶]Plateforme d'Imagerie Cellulaire, INSERM, Institut Fédératif de Recherche Necker Enfants-Malades (IFR94), Université Paris Descartes, 75014 Paris, France

Background: Endothelial cells secrete the hemostatic protein von Willebrand factor (VWF), stored in granules called Weibel-Palade bodies (WPBs).
Results: The scaffolding protein Discs large 1 (Dlg1) is in complex with clathrin, adaptator protein complex 1 (AP-1), and VWF. Its depletion impairs WPB formation.
Conclusion: Dlg1 participates in the AP-1/clathrin coat necessary for WPB biogenesis.
Significance: This study introduces a new Dlg1 function in exocytosis.

Weibel-Palade bodies (WPBs) are specific cigar-shaped granules that store von Willebrand factor (VWF) for its regulated secretion by endothelial cells. The first steps of the formation of these granules at the *trans*-Golgi network specifically require VWF aggregation and an external scaffolding complex that contains the adaptator protein complex 1 (AP-1) and clathrin. Discs large 1 (Dlg1) is generally considered to be a modular scaffolding protein implicated in the control of cell polarity in a large variety of cells by specific recruiting of receptors, channels, or signaling proteins to specialized zones of the plasma membrane. We propose here that in endothelial cells, Dlg1, in a complex with AP-1 and clathrin, participates in the biogenesis of WPBs. Supporting data show that Dlg1 colocalizes with microtubules, intermediate filaments, and Golgi markers. Tandem mass spectrometry experiments led to the identification of clathrin as an Dlg1-interacting partner. Interaction was confirmed by *in situ* proximity ligation assays. Furthermore, AP-1 and VWF immunoprecipitate and colocalize with Dlg1 in the juxtanuclear zone. Finally, Dlg1 depletion by siRNA duplexes disrupts *trans*-Golgi network morphology and WPB formation. Our results provide the first evidence for an unexpected role of Dlg1 in controlling the formation of specific secretory granules involved in VWF exocytosis in endothelial cells.

In *Drosophila*, the multidomain scaffolding proteins scribble (Scrib in mammals), discs large (Dlg), and lethal giant larvae (Lgl) form the Scrib polarity complex and act together to regulate epithelial cell apicobasal polarity. In particular, Dlg protein was shown to be located at septate junctions between epithelial cells and is required for the maintenance of junction structure and for the differential composition of basal and apical membranes (1). Dlg1, the mammalian orthologue of *Drosophila* Dlg, colocalizes with the adhesion molecule E-cadherin at the lateral sites of cell-cell contacts in mammary epithelial cells (2, 3). In these cells, Dlg1 depletion gave differing results, showing, depending on the authors, that Dlg1 loss may alter adherens junction integrity or tight junction function (4, 5). The contribution of Dlg1to the control of epithelial cell polarity is less clear in mammals than in *Drosophila*.

Endothelial cells are the only other cell type displaying an apicobasal polarity (6–9). The maintenance of this polarity is necessary for one of the major roles of endothelial cells, secretion by exocytosis of several proteins that regulate blood coagulation, blood flow, and local immune responses (10). Among them, the proinflammatory adhesive protein von Willebrand factor (VWF)[2] acts in the recruitment of platelets during blood vessel injury and in leukocyte extravasation (11–13). Von Willebrand's disease is the most common inherited bleeding disorder in humans, and the association between VWF and coronary heart disease is well documented (14, 15). More recently, VWF was proposed as a promising emerging target in stroke therapy (16).

VWF is stored, in endothelial cells, in unique large tubular granules (1–6 μm long, 0.1–0.3 μm in diameter) called Weibel-Palade bodies (WPBs) (17, 18). The elaborate biogenesis of these particular cigar-shaped granules is still under investigation (17). Although clathrin is known to provide an external scaffold to shape small, 50- to 100-nm transport vesicles, the formation of much larger, dense-cored secretory granules such as WPBs is driven by selective aggregation of soluble internal

[S] This article contains supplemental Fig. S1.

[1] To whom correspondence should be addressed: INSERM U698, Université Paris 7, Hemostasis, Bio-Engineering and Cardiovascular Remodeling, CHU X. Bichat, 46 rue Henri Huchard, 75018 Paris, France. Tel.: 33-1-40-25-75-22; Fax: 33-1-40-25-86-02; E-mail: laurence.walch@inserm.fr.

[2] The abbreviations used are: VWF, von Willebrand factor; WPBs, Weibel-Palade body; TGN, *trans*-Golgi network; HUVEC, human umbilical vascular endothelial cell; hCMEC/D3, human cerebral microvasculature endothelial cell(s) D3; PAR, partitioning defective; AP-1, adaptator protein complex 1; AMPAR, α-amino-3-hydroxy-5-methyl-4-isoxazole propionic acid-type glutamate receptor.

cargo (*i.e.* VWF for WPBs) at the *trans*-Golgi network (TGN). However, in contrast to other secretory granules, it was more recently shown that cargo aggregation alone is not sufficient to form WPBs or mucin-containing glue granules in *Drosophila* salivary glands. It was proposed that an external scaffold that contains adaptator protein complex 1 (AP-1) and clathrin is also essential for the biogenesis of these particular granules (19, 20).

In endothelial cells, the mechanisms controlling the formation and maintenance of apicobasal polarity and the polarized sorting of secretory granules and transport vesicles are poorly understood. We speculated, by analogy with epithelial cells, that Dlg1 could be involved in the regulation of endothelial cell-cell junctions and of apicobasal polarity. However, the microscopy data presented in this report show that Dlg1 is not localized at sites of cell-cell junctions in endothelial cells. Instead, Dlg1 is mostly found at locations corresponding to microtubules, intermediate filaments, and the Golgi apparatus. We used tandem mass spectrometry to identify putative endothelial-specific direct or indirect Dlg1-interacting partners. Clathrin heavy chain was the Dlg1 coimmunoprecipitated protein identified with the best score. Additionally, we show that AP-1 and VWF also immunoprecipitate and colocalize with Dlg1 in the juxtanuclear zone. Finally, in Dlg1-depleted cells, the formation of WPBs was impaired. Together, these data provide the first evidence that Dlg1, in association with clathrin and AP-1, may control the formation of WPBs at the TGN.

EXPERIMENTAL PROCEDURES

Antibodies—The following antibodies were used: monoclonal and polyclonal anti-Dlg1 (catalog nos. sc-9961 and sc-25661, respectively), anti-Scrib (catalog no. sc-28737), and anti-ZO-2 (catalog no. sc-11448) from Santa Cruz Biotechnology, Inc. (Santa Cruz, CA); anti-β-actin (catalog no. ab6276), anti-clathrin heavy chain (catalog no. ab21679), and anti-GM130 (catalog no. ab52649) from Abcam (Cambridge, MA); anti-VE-cadherin (catalog no. BMS158) from Bender MedSystems (Vienna, Austria); anti-E-cadherin (catalog no. 3195), anti-α/β-tubulin (catalog no. 2148), and anti-vimentin (catalog no. 5741) from Cell Signaling Technology, Inc. (Beverly, MA); anti-VWF (catalog no. A 0082) from DAKO (Glostrup, Denmark); anti-γ-adaptin (catalog no. A 4200), anti-talin (catalog no. HPA004748), and anti-TGOLN2 (catalog no. HPA012609) from Sigma; peroxidase-conjugated affiniPure goat anti-rabbit IgG (catalog no. 111-035-144) and anti-mouse IgG (catalog no. 115-035-146) from Jackson ImmunoResearch Laboratories, Inc. (West Grove, PA); and Alexa Fluor 488 goat anti-mouse IgG highly cross-adsorbed (catalog no. A11029), Alexa Fluor 488 goat anti-mouse IgG1 (catalog no. A21121), Alexa Fluor 555 goat anti-mouse IgG2b (catalog no. A21147), and Alexa Fluor 555 goat anti-rabbit IgG highly cross-adsorbed (catalog no. A21429) from Invitrogen.

Cell Cultures and Transient Transfections—Cells were cultured in an incubator at 37 °C with 5% CO_2. Normal primary human umbilical vascular endothelial cells (HUVECs) were maintained with endothelial cell growth medium 2 (Promocell, Heidelberg, Germany) supplemented with the endothelial cell growth medium supplement pack (Promocell) and an antibiotic mixture (PAA Laboratories): 5 units/ml penicillin, 0.5 μg/ml streptomycin, and 25 ng/ml amphotericin B. Immortalized human cerebral microvasculature endothelial cells D3 (hCMEC/D3) were a generous gift from Pierre-Olivier Couraud (INSERM U567, Paris, France) (21). Cells were grown in endothelial basal medium-2 (Lonza, Basel, Switzerland) supplemented with 5% (v/v) fetal calf serum (PAA Laboratories, Pasching, Austria), 10 mM HEPES (PAA Laboratories), 1.4 μM hydrocortisone (Sigma), 5 μg/ml ascorbic acid (Sigma), 1 ng/ml basic fibroblast growth factor (Millipore, Temecula, CA), and the antibiotic mixture (PAA Laboratories). Caco-2 cells were maintained with high-glucose DMEM, glutamax, and pyruvate (Life Technologies, Carlsbad, CA) and supplemented with 20% (v/v) fetal calf serum (PAA Laboratories) and the antibiotic mixture (PAA Laboratories). HUVECs and hCMEC/D3 were plated on rat tail type 1 collagen-coated (BD Biosciences) tissue culture dishes until passages 4 and 35, respectively. hCMEC/D3 were transfected with the custom Dlg1 siRNA duplexes N8 (sense sequence, GGACCAGAGUGAGCAGGAAtt) and N11 (GACAGACAGCUCAGAAGUUtt) or with the irrelevant siRNA duplex Neg (siRNA negative control, Eurogentec, Seraing, Belgium). The transfection reagent Lipofectamine 2000 (Life Technologies) was used as recommended by the supplier with slight modifications. Briefly, for a 6-well culture plate, a combination of 7.5 μl of Lipofectamine 2000 and 250 pmol of siRNA duplexes was added to each well.

Western Blotting—Samples in Laemmli buffer were separated by SDS-PAGE. Proteins were then transferred onto nitrocellulose membranes (Hybond-ECL, Amersham Biosciences) and membranes were blocked with TBS-Tween containing 5% (w/v) skimmed milk for 1 h at room temperature and then incubated overnight with the primary antibody (anti-β-actin, 0.42 μg/ml; anti-γ-adaptin, 1.5 μg/ml; anti-clathrin heavy chain, 1 μg/ml; anti-Dlg1, 1 μg/ml; anti-GM130, 42 pg/ml; anti-talin, 0.24 μg/ml; anti-α/β-tubulin, 40 pg/ml; anti-vimentin, 9 pg/ml; and anti-VWF, 3 μg/ml) at 4 °C under stirring. After washing with TBS-Tween, membranes were incubated with the suitable secondary antibody coupled to peroxidase, and immune complexes on the membranes were finally revealed by enhanced chemiluminescence (ECL+, Amersham Biosciences) and visualized by exposure to films (Hyperfilm ECL, Amersham Biosciences).

Immunoprecipitation—Cells were lysed in a hypotonic buffer (200 mM Hepes (pH 7.9), 15 mM $MgCl_2$, 100 mM KCl, supplemented with protease inhibitor cocktail and phosphatase inhibitor cocktails 2 and 3 (Sigma)). Then, 0.5% (v/v) Triton X-100 and 100 mM NaCl were added to the lysates, which were subsequently preclarified by centrifugation (10,000 × *g*, 4 °C, 10 min). Immunoprecipitation was performed by incubating 600 μg of proteins with 2 μg of primary antibody overnight at 4 °C under stirring. Irrelevant mouse IgG1 and rabbit IgG were used as controls. Magnetic beads (15 μl, Ademtech, Pessac, France) coupled to protein A or protein G were used to precipitate the immunocomplexes as recommended by the manufacturer. Immunoprecipitates were finally eluted from the beads by boiling for 5 min in an SDS-PAGE buffer containing β-mercaptoethanol. Samples were submitted to Western blot analysis.

Tandem Mass Spectrometry—Immunoprecipitated proteins were digested directly on beads overnight at 37 °C by sequencing grade trypsin (12.5 μg/ml, Promega, Madison, WI) in 20 μl of 25 mmol/liter NH_4HCO_3. Digests were analyzed by an LTQ Velos Orbitrap (Thermo Fisher Scientific, San Jose, CA) coupled to an Easy nano-LC Proxeon system (Thermo Fisher Scientific). Chromatographic separation of peptides was performed with the following parameters: column Easy Column Proxeon C18 (10 cm, 75 μm in inner diameter, 120 A), 300 nl/min flow, gradient rising from 95% solvent A (water, 0.1% formic acid) to 25% B (100% acetonitrile, 0.1% formic acid) in 20 min, then to 45% B in 40 min, and finally to 80% B in 10 min. Peptides were analyzed in the Orbitrap in full ion scan mode at a resolution of 30,000 and a mass range of 400–1800 *m*/*z*. Fragments were obtained with a collision-induced dissociation activation with a collisional energy of 40% and an activation Q of 0.250 for 10 ms and then analyzed in the LTQ. MS/MS data were acquired in a data-dependent mode in which the 20 most intense precursor ions were isolated with a dynamic exclusion of 20 s and an exclusion mass width of 10 ppm. Data were processed with Proteome Discoverer 1.2 software (Thermo Fisher Scientific) coupled to an in-house MASCOT search server (Matrix Science, Boston, MA, version 2.3.02). The mass tolerance of fragment ions was set to 10 ppm for precursor ions and 0.6 Dalton for fragments. The following modifications were used in variable modifications: oxidation (M) and phosphorylations (STY). The maximum number of missed cleavages was limited to two for trypsin digestion. MS-MS data were searched against SwissProt databases with the *Homo sapiens* taxonomy. A reversed database approach was used for the false discovery rate estimation. A threshold of 1% was chosen for this rate. Proteins with a MASCOT score higher than 45 were considered as clearly identified. Proteins identified in Dlg1 immunoprecipitates with a null score in the IgG1 control immunoprecipitates were considered as putative Dlg1 partners.

Immunocytochemistry—Cells were grown on 8-chamber Permanox Lab-Tek slides (Nalgene Nunc Corp., Rochester, NY) coated with rat tail collagen type 1 or on precoated collagen 1 coverslips (BD Biosciences). Cells were washed with PBS, supplemented with 1 mM Mg^{2+} and 1 mM Ca^{2+}, and fixed with 3.7% (w/v) paraformaldehyde in PBS for 15 min. The reaction was stopped with the addition of 50 mM NH_4Cl for 15 min. Finally, cells were blocked for 15 min with 0.5% (w/v) BSA and 0.1% (v/v) Triton X-100 in PBS. Wells were then incubated with the suitable primary antibody against γ-adaptin (3 μg/ml), E-cadherin (0.215 μg/ml), VE-cadherin (5 μg/ml), clathrin heavy chain (1 μg/ml), Dlg1 (10 μg/ml), GM130 (2.1 μg/ml), Scrib (10 μg/ml), TGOLN2 (0.53 μg/ml), α/β-tubulin (1.6 μg/ml), vimentin (0.18 μg/ml), VWF (2.6 μg/ml), and ZO-2 (2 μg/ml) for 1 h at room temperature. Negative control staining was performed using non-relevant IgG. After several washes in blocking buffer, cells were labeled with the appropriate Alexa Fluor fluorochrome-conjugated secondary antibody (4 μg/ml, Molecular Probes, Invitrogen) diluted in blocking buffer. F-actin was stained with Alexa Fluor 555-conjugated phalloidin (Invitrogen). Finally, slides were mounted in DAKOCytomation fluorescent mounting medium (DAKO), and cells were imaged using a fluorescent (Nikon, Kanagawa, Japan) or confocal microscope (LSM700 META, Zeiss). Colocalization and Pearson's correlation coefficients were determined using ImageJ software (National Institutes of Health, Bethesda, MD). Colocalization was indicated by a Pearson's coefficient ranging from 0.5–1 (22).

Duolink® in Situ Proximity Ligation Assay (PLA)—This technique is adapted from Soderberg and coworkers (23). Cells were labeled with a combination of primary antibodies as for immunocytochemistry and incubated with a pair of nucleotide-labeled secondary antibodies (rabbit PLA probe MINUS and mouse PLA probe PLUS, OLINK Biosciences, Uppsala, Sweden) diluted at 1:10 in saturation buffer for 2 h at room temperature. According to the instructions of the manufacturer, interactions between the PLA probes were revealed by addition of a hybridation solution consisting of two oligonucleotides that will hybridize to the two PLA probes if they are in close proximity (within a distance less than 40 nm), addition of a ligation solution joining the two hybridized oligonucleotides to form a closed circle, by amplification of the rolling-circle product using a polymerase and nucleotides, and, finally, by detection with hybridizing 563-labeled oligonucleotides. Cell nuclei were stained with 4′,6-diamino-2-phenylindole. Signals indicative of interactions were detected by confocal microscopy as small distinct fluorescent dots in visible red.

Isolation of Triton X-100-insoluble and Triton X-100-soluble Fractions—Cell fractionation was performed in accordance with a method described previously (24, 25). Cells were briefly washed twice with ice-cold PBS and scraped off for lysis by incubation, for 5 min at 4 °C under stirring, with 1% (v/v) Triton X-100, 100 mM Tris-HCl (pH 7.4), supplemented with protease inhibitor cocktail and phosphatase inhibitor cocktails 2 and 3 (Sigma). The large-size Triton X-100-insoluble fraction (cytoskeleton) was isolated by centrifugation at 15,600 × *g* at 4 °C for 4 min. To obtain the insoluble fraction of low size (cortical cytoskeleton), the Triton X-100-soluble fraction was further centrifuged at 100,000 × *g* for 4 h at 4 °C. The resulting supernatant represents the final Triton X-100-soluble fraction. The Triton X-100-insoluble fractions were solubilized by incubation, for 30 min at 4 °C under stirring with 1% (v/v) SDS and 100 mM Tris HCl (pH 7.4) supplemented with protease inhibitor cocktail and phosphatase inhibitor cocktails 2 and 3 (Sigma) and sonicated briefly. Protein concentration was determined in each sample using the BCA protein assay (Pierce). Finally, 20 or 5 μg of proteins was submitted to Western blotting.

Statistical Analysis—Values are expressed as mean ± S.E. The significance of differences between groups was tested using the Student's *t* test. A value of $p \leq 0.05$ was considered significant.

RESULTS

Expression and Localization of Dlg1 in Endothelial Cells—Epithelial and endothelial cells display an apicobasal polarity critical for many aspects of their functions. Polarity complexes, such as the Scrib complex, formed of Scrib, Dlg1, and Lgl, have been implicated in the formation and maintenance of the apicobasal polarity in epithelial cells. Less is known concerning the role of these complexes in endothelial cells. To establish whether Dlg1 is present at cell-cell contacts between endothe-

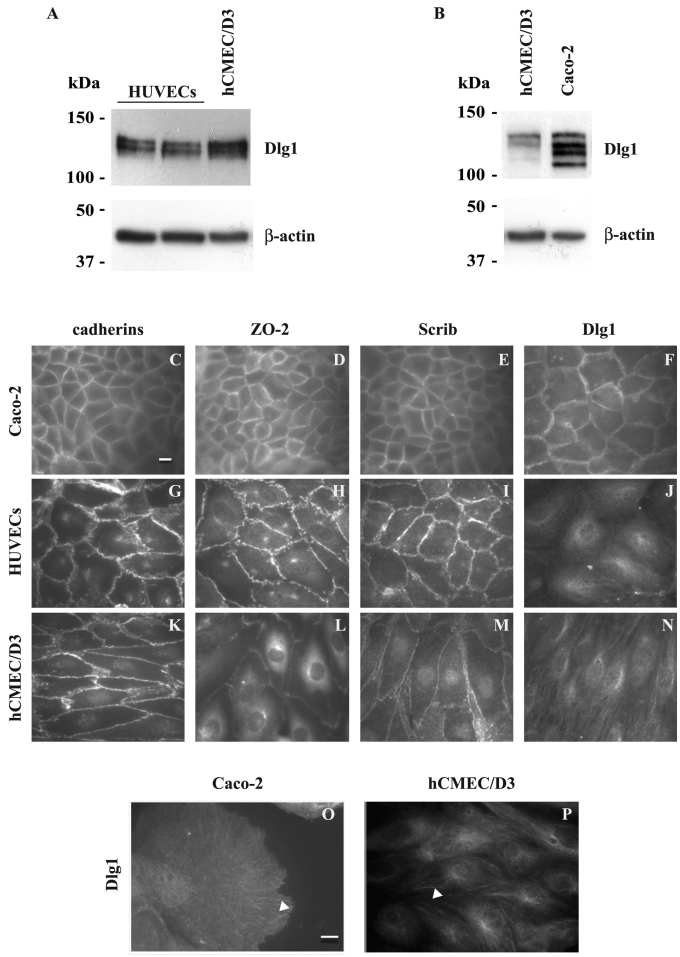

FIGURE 1. **In postconfluent endothelial cells, Dlg1 is not localized at sites of cell-cell junctions.** *A* and *B*, Dlg1 expression levels were compared by Western blotting in whole cell lysates of two different HUVEC cultures and of cultured hCMEC/D3 and Caco-2 cells. The same amounts of each postconfluent cell extract (20 μg protein) were loaded per lane. β-actin detection was used as a loading control. *C–N*, detection of the cell-cell junction markers E-cadherin (*C*), VE-cadherin (*G* and *K*), ZO-2 (*D*, *H*, and *L*), Scrib (*E*, *I*, and *M*) and Dlg1 (*F*, *J*, and *N*) by immunostaining of postconfluent Caco-2 cells, HUVECs, and hCMEC/D3. *O* and *P*, detection of Dlg1 by immunostaining of subconfluent Caco-2 cells and hCMEC/D3. Cells were imaged by epifluorescence microscopy. *Scale bar* = 10 μm. The *white arrowheads* indicate structures likely corresponding to the cytoskeleton.

lial cells as it is in epithelial cells, we compared Dlg1 localization in HUVECs and in hCMEC/D3 with its localization in human epithelial colorectal adenocarcinoma cells, the Caco-2 cell line. HUVECs are primary endothelial cells isolated from the human umbilical vein that are well characterized and used extensively in the literature. hCMEC/D3 is an immortalized human brain microvascular endothelial cell line, and these cells are considered as a model of the human blood-brain barrier (21). First, Western blotting data show that Dlg1 is expressed as a doublet in postconfluent HUVECs and hCMEC/D3 cells, whereas postconfluent Caco-2 cell cultures express four distinct forms of the protein (Fig. 1, *A* and *B*). This pattern of expression is similar whatever the state of cell confluency (data not shown). The comparative steady-state levels of Dlg1 were as follows: HUVECs < hCMEC/D3 < Caco-2. Then, to determine intracellular Dlg1 distribution, fixed postconfluent cells were submitted to immunostaining. The localization of cell-cell contact markers (cadherins, the tight junction-associated protein ZO-2, and Scrib) was also imaged to ascertain that mature cell junctions were fully established between cells. Although cell-cell contact markers, including Scrib, were present at the cell junctions in every cell type tested, Dlg1 was found in that localization only in Caco-2 cells (Fig. 1, *C–N*). In endothelial cells, Dlg1 showed a surprisingly diffuse staining with a filamentous aspect, more intense at the perinuclear region (Fig. 1, *J* and *N*). We were then interested to compare Dlg1 staining in subconfluent Caco-2 cells and hCMEC/D3 under conditions where mature cell-cell contacts are not established between cells (Fig. 1, *O* and *P*). Staining was similar in both cell types, with the labeling of tubular structures reminiscent of the cytoskeleton and emerging from the perinuclear area. These results suggest that Dlg1 localization in endothelial cells and subconfluent epithelial cells is likely due to a default of the recruitment of the protein by the cell-cell junction complexes. Finally, because Dlg1 expression was greater in hCMEC/D3 cells than in HUVECs, and because both cell types showed a similar intracellular distribution of the protein, further experiments were performed in hCMEC/D3.

To validate that Dlg1 is associated with the cytoskeleton in endothelial cells, we first isolated Triton X-100-insoluble (cytoskeleton) and Triton X-100-soluble fractions (membrane and cytosol) from postconfluent cultures of hCMEC/D3. The large-size (low-speed) insoluble fraction (*F1*) was particularly enriched with vimentin and Dlg1 (Fig. 2*A*). This fraction is also likely to contain a more stable pool of microtubules less sensitive to cold-induced depolymerization. The insoluble fraction of low size (high-speed, *F2*) was rich in talin, a focal adhesion protein, but poorer in Dlg1. Finally, the soluble fraction (*F3*) was rich in depolymerized α/β-tubulin and the poorest in Dlg1. β-Actin was present in all fractions with little variation. Consequently, fractionation data argue in favor of the association of the bulk of Dlg1 protein with the large size cytoskeleton. Supporting data were obtained by comparison of Dlg1 immunostaining with cytoskeletal marker staining in fixed hCMEC/D3. Confocal data show that Dlg1 partially colocalizes at the perinuclear region with α/β-tubulin (Pearson's correlation coefficient (r) = 0.613) and vimentin (r = 0.522), the markers of microtubules and intermediate filaments, respectively. In contrast, Dlg1 does not colocalize with actin stress fibers (r = 0.201, Fig. 2, *B–J*).

Identification of New Putative Partners of Dlg1 in Endothelial Cells—As a first step to elucidate the function of Dlg1 in endothelial cells, we sought for direct or indirect interacting partners. First, the pattern of the proteins, immunoprecipitated with the specific monoclonal Dlg1 antibody, in hCMEC/D3 whole cell lysates was compared with the pattern of the proteins immunoprecipitated with a nonspecific immunoglobulin, IgG1 (Fig. 3*A*). Results show a clear discrepancy between the two patterns, suggesting that the immunoprecipitation of Dlg1 together with its interacting partners is specific. Then, the proteins immunoprecipitated with Dlg1 were identified by tandem mass spectrometry after direct trypsinization (supplemental Fig. S1). Among the proteins successfully identified with a MASCOT score greater than 45 in the digested Dlg1 immunoprecipitates and a null score in the IgG1 immunoprecipitates

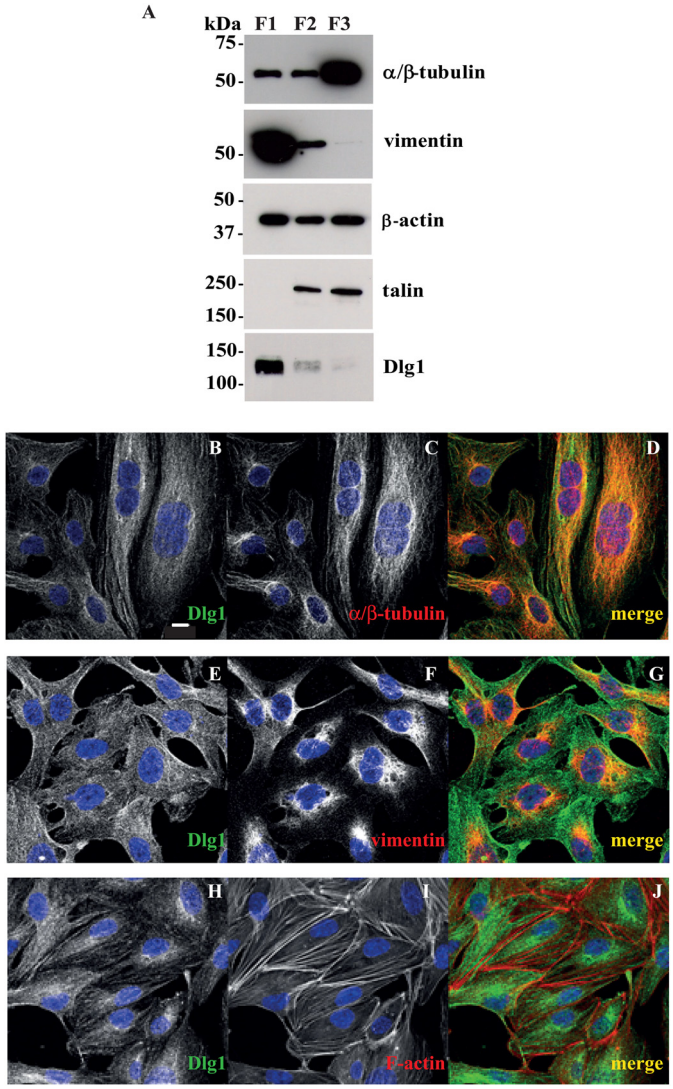

FIGURE 2. **In hCMEC/D3 cells, Dlg1 colocalizes with perinuclear components of microtubules (α/β-tubulin) and intermediate filaments (vimentin).** *A*, cytoskeletal and cortical cytoskeletal structures were separated from hCMEC/D3 total cell lysates as Triton X-100-insoluble fractions (low speed fraction (*F1*) and high speed fraction (*F2*), respectively). The Triton X-100-soluble fraction (*F3*) represents membranes and cytosol. Fractions were analyzed by Western blotting for the expression of Dlg1 and cytoskeletal markers (α/β-tubulin, vimentin, β-actin, and talin). 5 μg (α/β-tubulin, vimentin, and β-actin) or 20 μg (Dlg1 and talin) of protein were loaded in all lanes. An experiment representative of two independent ones is shown. *B–J*, hCMEC/D3 were stained for Dlg1 (*B*, *E*, and *H*, *green signal*) and cytoskeletal markers (*C*, α/β-tubulin; *F*, vimentin; and *I*, F-actin; *red signal*). *D*, *G*, and *J*, the image overlay (*merge*) was analyzed by confocal microscopy. Scale bar = 10 μm.

were the heavy chains of the microtubule-dependent motor protein kinesin-1 (MASCOT score = 68 ± 4) and of the coated vesicle component clathrin (Fig. 3*B*). Mass spectrometry identification of kinesin-1 as a putative Dlg1 partner was not confirmed because this protein was not detected by Western blotting in Dlg1 immunoprecipitates using two different antibodies (data not shown). In contrast, in hCMEC/D3 homogenates, specific monoclonal Dlg1 antibody was able to coimmunoprecipitate clathrin heavy chain, detected by Western blotting using specific polyclonal antibodies (Fig. 3*C*). Reciprocally, specific polyclonal clathrin antibodies were able to coimmunoprecipitate the shorter form of Dlg1 (Fig. 3*D*). Clathrin heavy chain was also detectable by Western blotting in Dlg1 immunoprecipitates derived from subconfluent Caco-2 cell lysates (Fig. 3*F*). To confirm that clathrin and Dlg1 may be present in the same protein complexes, the close proximity of the two endogenous proteins was tested by a Duolink® *in situ* PLA assay. PLA staining of clathrin and Dlg1, as well as of clathrin and the γ-adaptin subunit of AP-1 used as a positive control, revealed numerous dots in fixed hCMEC/D3, indicating that the couples of proteins are less than 40 nm apart (Fig. 3, *G* and *H*). In contrast, only a few PLA-positive dots were observed in cells labeled with the corresponding non-relevant immunoglobulins (Fig. 3, *I* and *J*). Therefore, these data confirm that in hCMEC/D3, clathrin and Dlg1 are directly or indirectly associated in complexes.

The association of Dlg1 with the perinuclear cytoskeleton and its interaction with clathrin led us to the hypothesis that, in endothelial cells, Dlg1 could be involved in secretory pathways. To test this hypothesis, we first investigated whether the clathrin-associated adaptator protein complex AP-1, which is known to mediate vesicle sorting from the TGN, may also be an interacting partner of Dlg1. Indeed, the γ-adaptin subunit of AP-1 detected by Western blotting coimmunoprecipitated with Dlg1 in hCMEC/D3 whole cell lysates, suggesting that AP-1 and Dlg1 are in a complex in endothelial cells (Fig. 3*E*).

To validate these coimmunoprecipitation data, protein colocalization was verified by confocal microscopy. Results show that Dlg1 and clathrin heavy chain as well as Dlg1 and γ-adaptin colocalize perinuclearly in hCMEC/D3 (Fig. 4, *A–H*). In addition, Dlg1 partly colocalizes with GM130, a *cis*-Golgi marker, and *trans*-Golgi network protein 2 (TGOLN2), a TGN marker (Fig. 4, *I–P*). Together, these results suggest that in endothelial cells, Dlg1 is complexed with the AP-1/clathrin coat of vesicles emerging from the TGN.

Effect of Dlg1 Depletion on TGN Morphology—Previous reports have shown that interference with cargo exit from the TGN may disturb Golgi morphology and may even lead to its dispersion. As Dlg1 in hCMEC/D3 is in complex with AP-1 and clathrin, which are necessary for the formation of exocrine secretory vesicles, we addressed whether Dlg1 depletion may lead to alteration of TGN structure. To reduce Dlg1 expression in hCMEC/D3, we used two siRNA duplexes, N8 and N11, directed against two different Dlg1 nucleotide sequences. Transfection with both siRNA duplexes led to a specific partial down-regulation of Dlg1 mRNA and protein (data not shown). However, N8 duplexes have a slight tendency to be more potent than N11 duplexes, with a resulting decrease in the steady-state Dlg1 level by 60% *versus* 50%, respectively. Transfection with the irrelevant siRNA duplexes was without significant effect on Dlg1 expression. Additionally, the global morphology, analyzed by white light microscopy, of transfected cells with any of the siRNAs used, was similar to the global morphology of control cells (data not shown).

To assess TGN morphology, we immunostained fixed cells for TGOLN2. Transfection with the siRNA duplex N8 may lead to the partial disorganization of the TGN (Fig. 5*C*). The number of non-mitotic cells with TGN dispersion was significantly greater in cell populations transfected with N8 siRNA duplexes than in non-transfected cells or those transfected with Neg

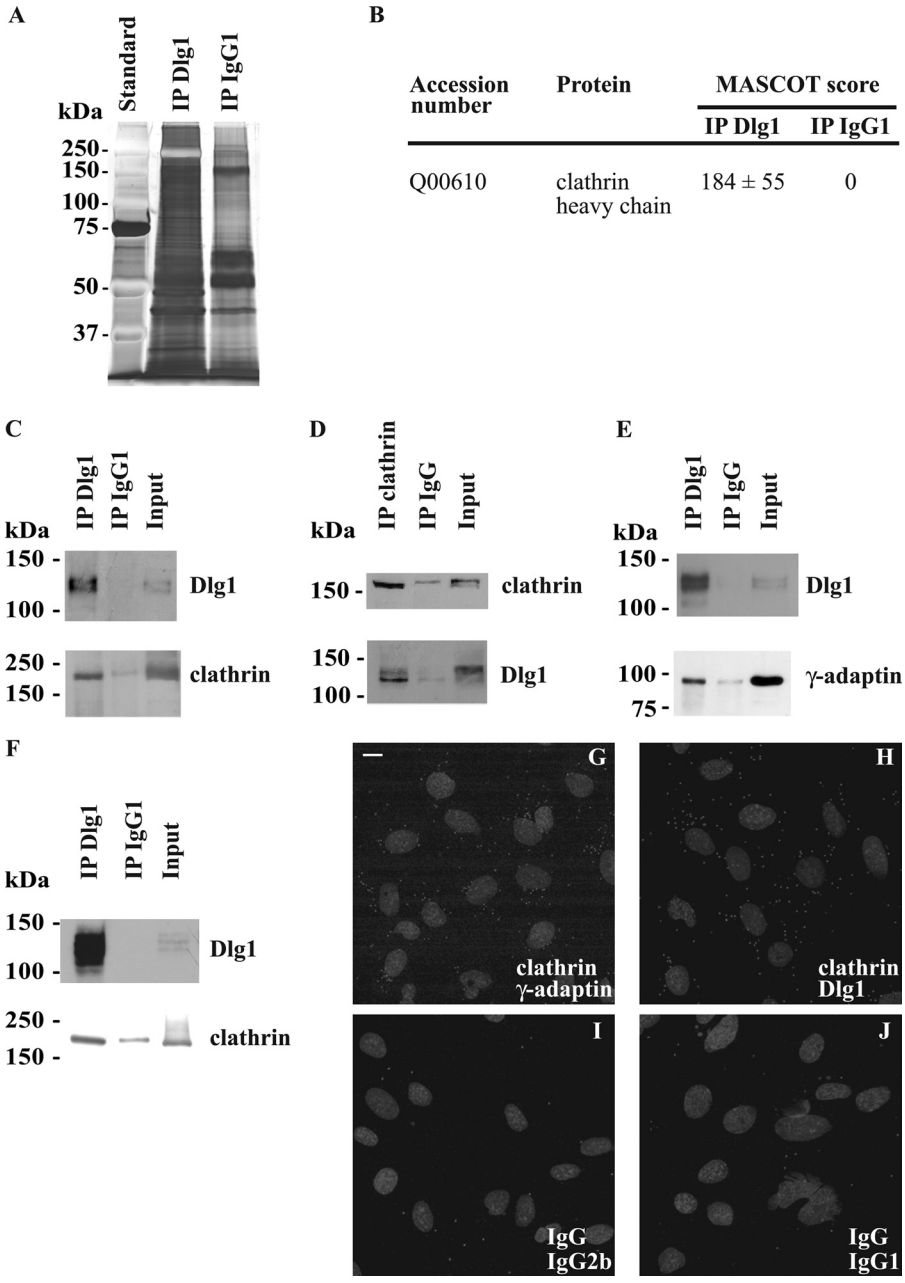

FIGURE 3. **Identification of the coated vesicle components, clathrin heavy chain, and the γ-adaptin subunit of AP-1 as putative direct or indirect Dlg1-interacting partners.** *A*, comparative patterns of the proteins immunoprecipitated from whole hCMEC/D3 lysates using monoclonal Dlg1 antibody (*IP Dlg1*) or a nonspecific immunoglobulin IgG1 (*IP IgG1*). Proteins were separated on an SDS-polyacrylamide gel and stained with silver nitrate. *B*, the proteins immunoprecipitated as mentioned above were trypsinized and identified by tandem mass spectrometry. Identified proteins with a MASCOT score higher than 45 in the IP Dlg1 sample and with a null score in the IP IgG1 sample are considered as putative Dlg1 partners. MASCOT scores are the means ± S.E. from three different experiments. *C* and *D*, the presence of clathrin heavy chain in Dlg1 immunoprecipitates was validated by Western blotting. Lysates derived from hCMEC/D3 were immunoprecipitated using a monoclonal Dlg1 antibody (*C*), a polyclonal clathrin heavy chain antibody (*D*), or a control IgG. Immunoprecipitates were subjected to Western blotting with Dlg1 or clathrin heavy chain-specific antibodies. *E*, AP-1 was tested as a Dlg1-interacting partner. Lysates were immunoprecipitated using a polyclonal Dlg1 antibody, and immunoprecipitates were subjected to Western blotting with monoclonal Dlg1 or γ-adaptin antibodies. *F*, lysates derived from subconfluent Caco-2 cells were immunoprecipitated using a monoclonal Dlg1 antibody or a control IgG1, and immunoprecipitates were subjected to Western blotting with clathrin heavy chain-specific antibodies. The input lane represents 3% of lysate used in immunoprecipitation reactions. *G–J*, Duolink® PLA labeling of fixed hCMEC/D3 using a polyclonal clathrin heavy chain antibody and a monoclonal γ-adaptin antibody (*G*) as a positive control to verify the *in situ* PLA procedure and a monoclonal Dlg1 antibody (*H*) or, as negative controls, an irrelevant rabbit immunoglobulin IgG and an irrelevant mouse immunoglobulin IgG2b (*I*) and irrelevant mouse immunoglobulin IgG1 (*J*). *Small gray dots* represent the PLA-positive signal. Nuclei appear as *gray ellipsoidal organelles*. An experiment representative of three independent ones is shown. *Scale bar* = 10 μm.

siRNA duplexes (Fig. 5*D*). The results provide indirect evidence that Dlg1 contributes to protein sorting at the TGN in endothelial cells.

Effect of Dlg1 Depletion on WPB Biogenesis—Because clathrin and AP-1 were shown previously to be essential for the initial steps of the formation of WPBs, the regulated VWF secretory granules in endothelial cells, we speculated that their new interacting partner, Dlg1, may also participate in WPB biogenesis. To address this hypothesis, Dlg1 and VWF expression were compared in the three Triton X-100 (in)soluble fractions

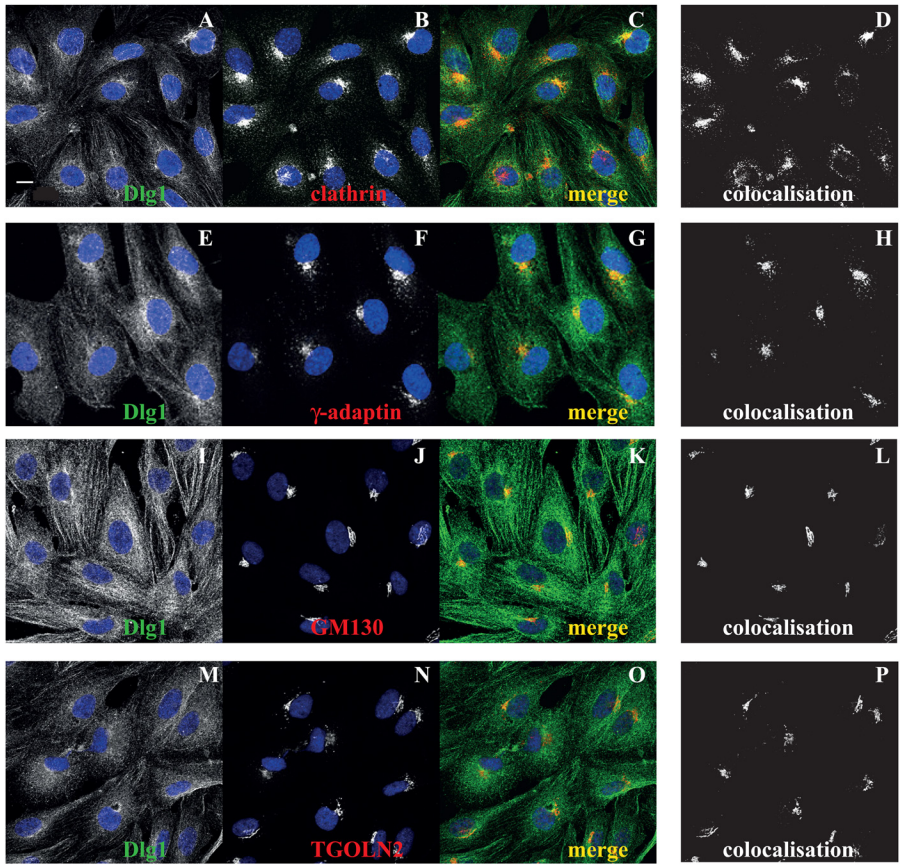

FIGURE 4. **Dlg1 colocalizes with perinuclear clathrin heavy chain and γ-adaptin in addition to the *cis*- and *trans*-Golgi markers GM130 and TGOLN2, respectively.** hCMEC/D3 were fixed and stained for Dlg1 (*A*, *E*, *I*, and *M*, *green signal*) and coated vesicle components or Golgi markers (*B*, clathrin; *F*, γ-adaptin; *J*, GM130; or *N*, TGOLN2; *red signal*). *C*, *G*, *K*, and *O*, the image overlay (*merge*) was analyzed by confocal microscopy. *D*, *H*, *L*, and *P*, colocalization was determined using ImageJ software. *Scale bar* = 10 μm.

obtained from hCMEC/D3 whole cell lysates (Fig. 6*A*). Two immunoreactive proteins were detected with the VWF antibody, a protein of an ~360-kDa apparent molecular weight, corresponding to the VWF precursor proVWF, and a protein of ~260 kDa, corresponding to mature VWF (26, 27). The bulk of both proteins was detected predominantly in the large-size (low-speed) insoluble fraction (F1), as was Dlg1. More generally, the pattern of expression of both Dlg1 and VWF were similar in all three fractions (Fig. 6*A*). The presence of most of the VWF signal in the Triton X-100-insoluble material has already been described by Giblin and coworkers (26). In fact, WPBs are resistant to 1% Triton X-100 for 5 min (data not shown), and, therefore, VWF is not extracted from its storage granules in these conditions. Then Dlg1 was immunoprecipitated from whole cell lysates followed by Western blotting detection of VWF (Fig. 6*B*). Data suggest that the mature form of VWF specifically coimmunoprecipitates with Dlg1 and not with the irrelevant IgG. In addition, Dlg1 and VWF localization was imaged by confocal microscopy (Fig. 6*C*). Dlg1 and VWF partially colocalize in a very discrete juxtanuclear zone. This colabeling was similar to that obtained for Dlg1 and TGOLN2 (Fig. 4*P*). Together, these data suggest that, in endothelial cells, Dlg1 and VWF are in a complex at the TGN. Finally, VWF immunostaining was analyzed in cells depleted for Dlg1. In fixed hCMEC/D3 not transfected or transfected with the irrelevant Neg siRNA duplexes, VWF is localized at WPBs all around the cells and also visualized as a diffuse labeling, which was likely to be localized at the endoplasmic reticulum (Fig. 7*A*). In hCMEC/D3 transfected with N8 or N11 siRNA duplexes, VWF labeling also appeared as perinuclear puncta (Fig. 7*B*). The number of cells with an accumulation of perinuclear puncta was counted in each condition (Fig. 7*C*). This number was greater in cells transfected with N8 and N11 siRNA duplexes as compared with control cells or cells transfected with Neg siRNA duplexes. In addition, although differences are not significant, this increase had a tendency to correlate with the extent of Dlg1 extinction obtained by the different Dlg1 siRNA duplexes (Fig. 7*C*). The effect of N8 and N11 duplexes in hCMEC/D3 was a phenocopy of the effect of AP-1 knockdown in a previous model of VWF-transfected HEK293 cells, which led to failure in WPB formation (20). Together, these data suggest that Dlg1 depletion impaired WPB formation in hCMEC/D3.

DISCUSSION

The results presented here show that in postconfluent cultured endothelial cells, Dlg1 is unexpectedly and mainly associated with the intracellular cytoskeleton and Golgi apparatus, even under conditions in which cell-cell junctions are well established. As an approach to elucidating Dlg1 endothelial function, we have identified three new putative Dlg1-interacting partners, clathrin, AP-1, and VWF. Functional data lead us

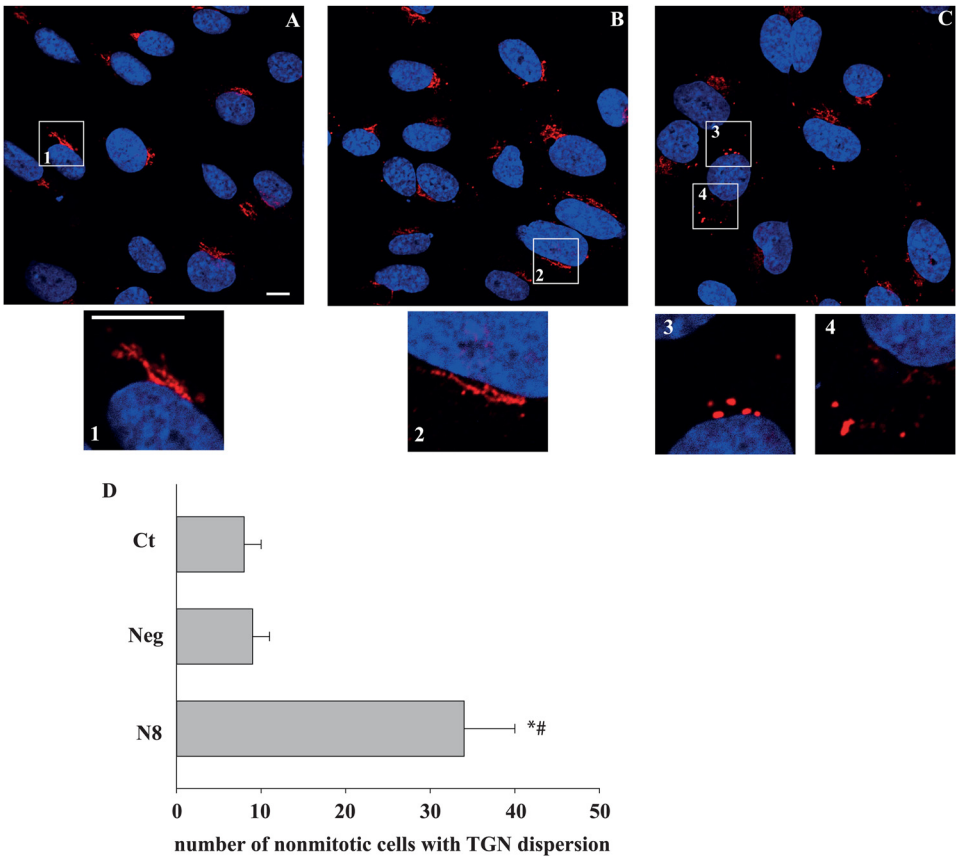

FIGURE 5. **Dlg1 depletion affects TGN morphology.** Three days post-transfection, hCMEC/D3, in control conditions (*A*) or treated with the siRNA duplexes Neg (*B*) or N8 (*C*), were fixed and stained for TGOLN2 (*red signal*). Cells were imaged using confocal microscopy. Digital zoom *panels 1* and *2* highlight TGOLN2-positive staining in control cells. *Panels 3* and *4* illustrate one representative cell, a punctiform staining positive for TGOLN2, suggesting partial TGN dispersion. *Scale bars* = 10 μm. *D*, hCMEC/D3 cells were transfected with Dlg1 siRNA duplexes, N8, or Neg-irrelevant siRNA duplexes or not transfected (*ct*). Three days post-transfection, cells were fixed and stained for TGOLN2 and then analyzed by epifluorescence microscopy. The number of nonmitotic cells with TGN dispersion was counted for each experiment among a total of 329 ± 23 cells/condition. Results are the mean ± S.E. from three different experiments. *, $p \leq 0.05$ *versus* non-transfected cells; #, $p \leq 0.05$ *versus* cells transfected with Neg siRNA duplexes.

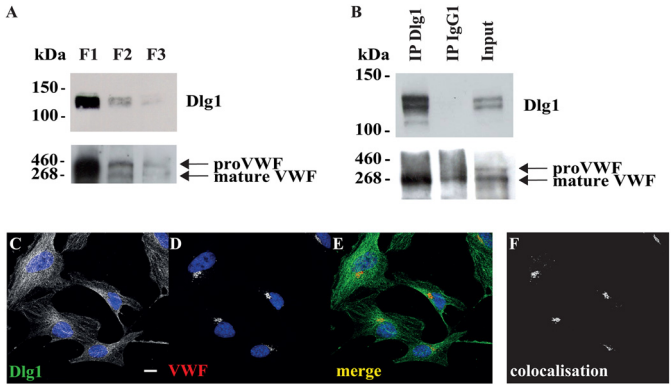

FIGURE 6. **VWF coimmunoprecipitates and colocalizes with Dlg1 in hCMEC/D3.** *A*, total cell lysates were separated as Triton X-100-insoluble fractions (low speed, fraction *F1* and high speed, fraction *F2*) and Triton X-100-soluble fraction (*F3*). Fractions were analyzed by Western blotting for the expression of Dlg1 and VWF. 20 μg of protein was loaded per lane. *B*, lysates were immunoprecipitated (*IP*) using a monoclonal Dlg1 antibody or a control IgG1. Immunoprecipitates were subjected to Western blotting with Dlg1 or VWF-specific antibodies. The *input* lane represents 3% of lysate used in immunoprecipitation reactions. An experiment representative of two independent ones is shown. *C–F*, cells were fixed and stained for Dlg1 (*C*, *green signal*) and VWF (*D*, *red signal*). *E*, the image overlay (*merge*) was analyzed by confocal microscopy. *F*, colocalization was determined using ImageJ software. *Scale bar* = 10 μm.

to suggest that in endothelial cells, Dlg1, together with clathrin and AP-1, may play a key role in the early stages of WPB formation at the TGN.

As a scaffolding protein, the subcellular localization of Dlg1 depends on its recruitment by molecular partners. Therefore, Dlg1 localization varies between cell types. In confluent mammalian epithelial cells, the localization of Dlg1 at lateral cell-cell junctions depends on its indirect interaction with E-cadherin (2). In endothelial cells, adherent junctions implicate the related VE-cadherin. However, in postconfluent HUVECs and hCMEC/D3, with well established cell-cell junctions as shown by the recruitment of the scaffolding proteins ZO-2 and Scrib, Dlg1 did not colocalize with junction markers (Fig. 1, *C–N*). Instead, we show that Dlg1 is present in Triton X-100-insoluble, low-speed fractions of hCMEC/D3 lysates (*i.e.* large-size cytoskeleton fraction) and by confocal microscopy is visualized to colocalize with microtubules, intermediate filaments, and Golgi markers (Figs. 2 and 4). Dlg1 has been described, together with Scrib and Lgl, as a constituent of the polarity complex called Scrib. Our results suggest that the distribution of Dlg1 but not Scrib differ between epithelial and endothelial cells. The distribution and composition of another cell polarity complex, the partitioning defective (PAR) complex, has already been shown to differ between epithelial and endothelial cells. In

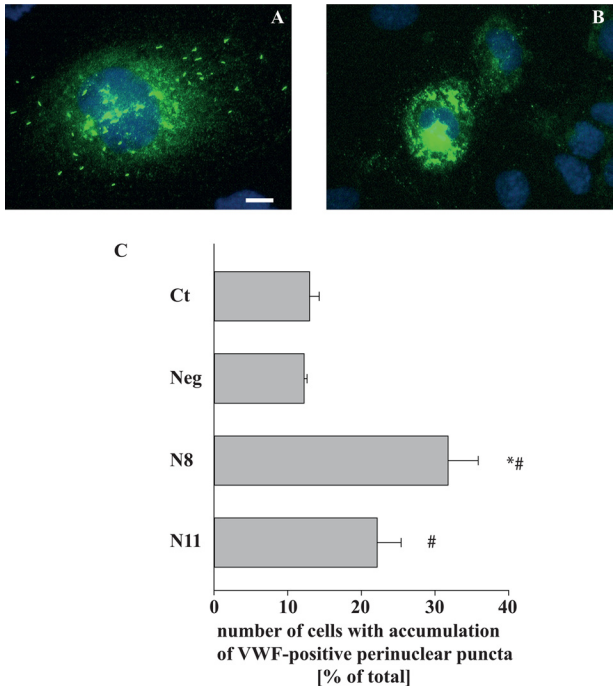

FIGURE 7. **Dlg1 depletion impairs WPB formation.** *A* and *B*, hCMEC/D3 were transfected with irrelevant Neg siRNA duplexes (*A*) or with N8 siRNA duplexes (*B*). Three days post-transfection, cells were fixed and immunolabeled for VWF (*green signal*). Cells were analyzed by epifluorescence microscopy. *Scale bar* = 10 μm. *C*, hCMEC/D3 were transfected with Dlg1 siRNA duplexes, N8 or N11, with Neg irrelevant siRNA duplexes, or not transfected (*ct*). Three days post-transfection, cells were fixed and stained for VWF. Cells were analyzed by epifluorescence microscopy. The number of cells with perinuclear VWF-positive puncta was counted for each experiment among a total of 194 ± 10 cells/condition. Results are the mean ± S.E. from three different experiments. *, $p \leq 0.05$ *versus* non-transfected cells; #, $p \leq 0.05$ *versus* cells transfected with Neg siRNA duplexes.

endothelial cells, a complex consisting of the association of the scaffolding proteins PAR-3 and PAR-6 was shown to be directly associated with VE-cadherin, whereas in epithelial cells, the PAR-3/atypical protein kinase C/PAR-6 complex is localized to tight junctions and has a central role in the development of apicobasal polarity (28). The fine mechanisms that control apicobasal polarity in both cell types are, therefore, likely to be distinct.

Data show that, whatever their state of confluency, two main Dlg1 isoforms are expressed in endothelial cells, whereas, as previously shown, four main isoforms (an additional band just barely detectable may also be seen at longer exposure time) are expressed in Caco-2 cells (Fig. 1, *A* and *B*) (4). Isoforms are due to the presence of two small sites of alternatively spliced insertions in the Dlg1 coding sequence. The resulting functional consequences are still poorly understood (4). Because in subconfluent Caco-2 cells Dlg1 staining is similar to that in endothelial cells, revealing tubular structures resembling the cytoskeleton (Fig. 1, *O* and *P*), the discrepancy between Dlg1 subcellular localization in postconfluent epithelial and endothelial cells is not likely to be due to the differences noted in the expression of Dlg1 isoforms (Fig. 1, *A* and *B*). The data rather suggest that Dlg1 localization at cytoskeletal structures is due to an interaction with cytoskeleton-associated proteins combined with a defect in Dlg1 recruitment by cadherin complexes, independently of which Dlg1 isoforms are expressed.

A large number of cytoskeleton-associated proteins are direct or indirect partners of Dlg1 in a variety of cells. For example, among microtubule-associated proteins are the motor protein dynein, motors of the kinesin superfamily, and adenomatous polyposis coli, a protein associated with microtubule plus ends at the leading edge of migrating astrocytes (29–32). We show that Dlg1 is largely associated with perinuclear microtubules in endothelial cells (Fig. 2, *B–D*). Because its known microtubule-associated partners in other cell types may not be informative of Dlg1 functions in endothelial cells, we decided to perform a proteomic analysis to identify Dlg1 endothelial-specific interactants. Three microtubule-associated proteins were identified by tandem mass spectrometry in Dlg1 immunoprecipitates derived from hCMEC/D3 cells (microtubule-associated protein RP/EB family member 1, cytoplasmic dynein 1 heavy chain, and kinesin-1 heavy chain, supplemental Fig. S1). Among them, kinesin-1 was the only protein identified with a mean MASCOT score higher than 45, which was the *a priori* threshold that we had set to consider a protein as a potential Dlg1 partner. However, we failed to confirm kinesin-1 identification in Dlg1 immunoprecipitates by performing Western blotting (data not shown). Therefore, the cytoskeleton-associated proteins that are Dlg1 partners in endothelial cells remain to be established.

Given its role in protein trafficking and its identification with the most elevated MASCOT score (Fig. 3*B*), clathrin was the next putative Dlg1 partner in endothelial cells that caught our attention. In hCMEC/D3, the combination of Duolink® *in situ* PLA with coimmunoprecipitation shows that some of the endogenous clathrin and Dlg1 proteins are present in complexes (Fig. 3). Furthermore, the two proteins mainly colocalize in a juxtanuclear zone probably corresponding to the Golgi apparatus (Fig. 4). Among clathrin adaptators, which link clathrin to membrane components, are the AP complexes (33). The AP-2 complex is involved in clathrin-mediated endocytosis. AP-2 has been shown to exist in a complex with Dlg1, myosin VI, and α-amino-3-hydroxy-5-methyl-4-isoxazole propionic acid-type glutamate receptors (AMPARs) in rat brain (34). Dlg1 is thus suspected to participate in AMPAR endocytosis at the stimulated synapses. Similarly, the AP-1 complex is involved in clathrin-mediated vesicle sorting from the TGN to endosomes. By analogy with Dlg1 interaction with AP-2, we reasoned that AP-1 could be present in a complex with clathrin and Dlg1 in endothelial cells. In fact, Dlg1 and AP-1 coimmunoprecipitate and colocalize in hCMEC/D3 cells in a discrete zone adjacent to the nucleus, suggesting that Dlg1 may participate in the formation of AP-1/clathrin-coated vesicles at the TGN. Finally, the specific polyclonal clathrin antibodies coimmunoprecipitate only the shorter form of Dlg1, suggesting an isoform specificity in the interaction between clathrin and Dlg1 (Fig. 3*D*). As already shown in other cell types derived from the cardiovascular system, *i.e.* smooth muscle cells and cardiomyocytes, the larger and the shorter isoforms of Dlg1 differ, in endothelial cells, by an N-terminal insertion of a small proline-rich sequence named I1A that is due to the presence of a site of alternative splicing in the mRNA (data not shown) (35, 36). In the larger form, an SH3 binding site is thus present that may bind the SH3 domain of a number of protein tyrosine kinases or

of Dlg1 itself in an intra- or an extramolecular way that favors a "closed state" or the homomultimerization of the protein, respectively (37). The presence of the I1A insertion in Dlg1 is likely to inhibit the formation of protein complexes containing clathrin by causing interactions that would mask the required binding sites.

Previous reports have shown that impairment of clathrin-coated vesicle trafficking from the TGN, by depletion of a variety of proteins such as clathrin, the motor proteins myosin 1b and myosin 6, or Hip1R, which coordinate actin assembly with clathrin budding, leads to the swelling of Golgi cisternae and, therefore, to the perturbation of TGN morphology (38–41). As indirect evidence of Dlg1 implication in clathrin function, the data presented here show that Dlg1 depletion in hCMEC/D3 induces the loss of TGN structure (Fig. 5). In particular, the partial TGN dispersion observed in 35% of cells treated with N8 duplexes (Fig. 5*C*) is a phenocopy of the effect obtained on TGN morphology by Hip1R knockdown in HeLa cells (39).

Few WPB components have been identified so far, and the mechanisms of the early steps of WPB biogenesis are far from elucidation (17). Besides VWF aggregation, the presence of an AP-1/clathrin coat has been found to be essential for WPB formation (20). Interference with AP-1/clathrin function prevents the formation of WPBs at the TGN that instead become small and rounded puncta. Although the question of how a luminal soluble cargo (VWF) might interact with an external protein complex (AP-1/clathrin) remains to be answered, it was proposed that the AP-1/clathrin coat may specifically stabilize the initial folding of VWF into tubular aggregates (17, 20). AP-1 has relatively few known effectors. Recently the small GTPases Rab10 and Rab8 were shown to genetically interact with AP-1 and act in WPB formation at the level of the Golgi apparatus (27, 42). However, data is still lacking to develop a model that would explain WPB formation by integrating all partners already identified. We provide here the first evidence suggesting that Dlg1 is also an AP-1 partner and thus participates in the control of the early steps of WPB biogenesis. Firstly, in hCMEC/D3 lysates, Dlg1 immunoprecipitates with the mature form of VWF (Fig. 6*B*). The cleavage of the VWF prosequence occurs at the TGN, and therefore, the proVWF is mostly present in the endoplasmic reticulum and Golgi apparatus (26, 27, 43). Because Dlg1 and VWF colocalize in a discrete juxtaperinuclear zone reminiscent of the TGN (Fig. 6, *C–F*) and Dlg1 does not localize to WPBs, data suggest that Dlg1 and VWF are in a complex at the early stages of WPB formation. Secondly, Dlg1 depletion in hCMEC/D3, as shown previously in cells depleted for AP-1, causes an accumulation of small and rounded VWF-positive perinuclear puncta to the detriment of the normal cigar-shaped WPBs (Fig. 7). Finally, as already discussed, Dlg1 coimmunoprecipitates and colocalizes with clathrin and AP-1 in a juxtanuclear position. In a more speculative way, because Dlg1 interacts with the AP-1/clathrin complex, which forms an external coat to vesicles, and with the soluble internal cargo, VWF, it is likely that Dlg1 is associated with a yet-unidentified transmembrane protein that would be the missing link between VWF and the AP-1/clathrin complex.

The data presented here finally raise the question as to whether, more generally, although the biogenesis of the WPBs is very specific, the AP-1/clathrin/Dlg1 complex could also participate in the formation of transport vesicles necessary for the targeting of other substrates, such as receptors or channels, to the plasma membrane in endothelial cells as well as in other cell types. This hypothesis is supported by the observation that clathrin coimmunoprecipitates with Dlg1 in subconfluent epithelial cells (Fig. 3*F*), although, to our knowledge there is no evidence to date for a role of Dlg1 in Golgi-mediated exocytosis in these cells. In neurons, direct interaction of Dlg1 with AMPARs and the voltage-gated potassium channel Kv4.2 occurs very early in their biosynthetic pathway, while they are in the endoplasmic reticulum and the *cis*-Golgi network (44, 45). Furthermore, Dlg1 was shown to be involved in the trafficking of these receptors from the TGN to the postsynaptic compartment in association with the motor protein myosin VI. By analogy with Dlg1 interaction with AP-2 and the involvement in AMPAR endocytosis, we cannot exclude that Dlg1 may also participate, together with AP-1 and clathrin, in the formation AMPAR and Kv4.2 sorting vesicles (44, 46). It would be of interest to investigate whether the functional complex AP-1/clathrin/Dlg1 that we introduce here may contribute to shape transport vesicles or whether this complex is unique to the formation of the specific secretory granules, WPBs, in endothelial cells.

Acknowledgments—We thank Mary Pellegrin-Osborne for editorial assistance.

REFERENCES

1. Woods, D. F., Hough, C., Peel, D., Callaini, G., and Bryant, P. J. (1996) Dlg protein is required for junction structure, cell polarity, and proliferation control in *Drosophila* epithelia. *J. Cell Biol.* **134,** 1469–1482
2. Reuver, S. M., and Garner, C. C. (1998) E-cadherin mediated cell adhesion recruits SAP97 into the cortical cytoskeleton. *J. Cell Sci.* **111,** 1071–1080
3. Wu, H., Reuver, S. M., Kuhlendahl, S., Chung, W. J., and Garner, C. C. (1998) Subcellular targeting and cytoskeletal attachment of SAP97 to the epithelial lateral membrane. *J. Cell Sci.* **111,** 2365–2376
4. Laprise, P., Viel, A., and Rivard, N. (2004) Human homolog of disc-large is required for adherens junction assembly and differentiation of human intestinal epithelial cells. *J. Biol. Chem.* **279,** 10157–10166
5. Stucke, V. M., Timmerman, E., Vandekerckhove, J., Gevaert, K., and Hall, A. (2007) The MAGUK protein MPP7 binds to the polarity protein hDlg1 and facilitates epithelial tight junction formation. *Mol. Biol. Cell* **18,** 1744–1755
6. Horvat, R., Hovorka, A., Dekan, G., Poczewski, H., and Kerjaschki, D. (1986) Endothelial cell membranes contain podocalyxin, the major sialoprotein of visceral glomerular epithelial cells. *J. Cell Biol.* **102,** 484–491
7. Muller, W. A., and Gimbrone, M. A., Jr. (1986) Plasmalemmal proteins of cultured vascular endothelial cells exhibit apical-basal polarity. Analysis by surface-selective iodination. *J. Cell Biol.* **103,** 2389–2402
8. Nakache, M., Schreiber, A. B., Gaub, H., and McConnell, H. M. (1985) Heterogeneity of membrane phospholipid mobility in endothelial cells depends on cell substrate. *Nature* **317,** 75–77
9. Simionescu, N., Simionescu, M., and Palade, G. E. (1981) Differentiated microdomains on the luminal surface of the capillary endothelium. I. Preferential distribution of anionic sites. *J. Cell Biol.* **90,** 605–613
10. Sporn, L. A., Marder, V. J., and Wagner, D. D. (1989) Differing polarity of the constitutive and regulated secretory pathways for von Willebrand factor in endothelial cells. *J. Cell Biol.* **108,** 1283–1289
11. Petri, B., Broermann, A., Li, H., Khandoga, A. G., Zarbock, A., Krombach, F., Goerge, T., Schneider, S. W., Jones, C., Nieswandt, B., Wild, M. K., and Vestweber, D. (2010) von Willebrand factor promotes leukocyte extrava-

sation. *Blood* **116,** 4712–4719
12. Tschopp, T. B., Weiss, H. J., and Baumgartner, H. R. (1974) Decreased adhesion of platelets to subendothelium in von Willebrand's disease. *J. Lab. Clin. Med.* **83,** 296–300
13. Turitto, V. T., Weiss, H. J., Zimmerman, T. S., and Sussman, I. I. (1985) Factor VIII/von Willebrand factor in subendothelium mediates platelet adhesion. *Blood* **65,** 823–831
14. Blombäck, M., Eikenboom, J., Lane, D., Denis, C., and Lillicrap, D. (2012) von Willebrand disease biology. *Haemophilia* **18,** 141–147
15. Spiel, A. O., Gilbert, J. C., and Jilma, B. (2008) von Willebrand factor in cardiovascular disease. Focus on acute coronary syndromes. *Circulation* **117,** 1449–1459
16. De Meyer, S. F., Stoll, G., Wagner, D. D., and Kleinschnitz, C. (2012) von Willebrand factor. An emerging target in stroke therapy. *Stroke* **43,** 599–606
17. Metcalf, D. J., Nightingale, T. D., Zenner, H. L., Lui-Roberts, W. W., and Cutler, D. F. (2008) Formation and function of Weibel-Palade bodies. *J. Cell Sci.* **121,** 19–27
18. Weibel, E. R., and Palade, G. E. (1964) New Cytoplasmic components in arterial endothelia. *J. Cell Biol.* **23,** 101–112
19. Burgess, J., Jauregui, M., Tan, J., Rollins, J., Lallet, S., Leventis, P. A., Boulianne, G. L., Chang, H. C., Le Borgne, R., Krämer, H., and Brill, J. A. (2011) AP-1 and clathrin are essential for secretory granule biogenesis in *Drosophila*. *Mol. Biol. Cell* **22,** 2094–2105
20. Lui-Roberts, W. W., Collinson, L. M., Hewlett, L. J., Michaux, G., and Cutler, D. F. (2005) An AP-1/clathrin coat plays a novel and essential role in forming the Weibel-Palade bodies of endothelial cells. *J. Cell Biol.* **170,** 627–636
21. Weksler, B. B., Subileau, E. A., Perrière, N., Charneau, P., Holloway, K., Leveque, M., Tricoire-Leignel, H., Nicotra, A., Bourdoulous, S., Turowski, P., Male, D. K., Roux, F., Greenwood, J., Romero, I. A., and Couraud, P. O. (2005) Blood-brain barrier-specific properties of a human adult brain endothelial cell line. *FASEB J.* **19,** 1872–1874
22. Bolte, S., and Cordelières, F. P. (2006) A guided tour into subcellular colocalization analysis in light microscopy. *J. Microsc.* **224,** 213–232
23. Söderberg, O., Gullberg, M., Jarvius, M., Ridderstråle, K., Leuchowius, K. J., Jarvius, J., Wester, K., Hydbring, P., Bahram, F., Larsson, L. G., and Landegren, U. (2006) Direct observation of individual endogenous protein complexes in situ by proximity ligation. *Nat. Methods* **3,** 995–1000
24. Fox, J. E. (1985) Linkage of a membrane skeleton to integral membrane glycoproteins in human platelets. Identification of one of the glycoproteins as glycoprotein Ib. *J. Clin. Invest.* **76,** 1673–1683
25. Tamaru, S., Fukuta, T., Kaibuchi, K., Matsuoka, Y., Shiku, H., and Nishikawa, M. (2005) Rho-kinase induces association of adducin with the cytoskeleton in platelet activation. *Biochem. Biophys. Res. Commun.* **332,** 347–351
26. Giblin, J. P., Hewlett, L. J., and Hannah, M. J. (2008) Basal secretion of von Willebrand factor from human endothelial cells. *Blood* **112,** 957–964
27. Wagner, D. D. (1990) Cell biology of von Willebrand factor. *Annu. Rev. Cell Biol.* **6,** 217–246
28. Iden, S., Rehder, D., August, B., Suzuki, A., Wolburg-Buchholz, K., Wolburg, H., Ohno, S., Behrens, J., Vestweber, D., and Ebnet, K. (2006) A distinct PAR complex associates physically with VE-cadherin in vertebrate endothelial cells. *EMBO Rep.* **7,** 1239–1246
29. Etienne-Manneville, S., Manneville, J. B., Nicholls, S., Ferenczi, M. A., and Hall, A. (2005) Cdc42 and Par6-PKCζ regulate the spatially localized association of Dlg1 and APC to control cell polarization. *J. Cell Biol.* **170,** 895–901
30. Hanada, T., Lin, L., Tibaldi, E. V., Reinherz, E. L., and Chishti, A. H. (2000) GAKIN, a novel kinesin-like protein associates with the human homologue of the *Drosophila* discs large tumor suppressor in T lymphocytes. *J. Biol. Chem.* **275,** 28774–28784
31. Jeyifous, O., Waites, C. L., Specht, C. G., Fujisawa, S., Schubert, M., Lin, E. I., Marshall, J., Aoki, C., de Silva, T., Montgomery, J. M., Garner, C. C., and Green, W. N. (2009) SAP97 and CASK mediate sorting of NMDA receptors through a previously unknown secretory pathway. *Nat. Neurosci.* **12,** 1011–1019
32. Manneville, J. B., Jehanno, M., and Etienne-Manneville, S. (2010) Dlg1 binds GKAP to control dynein association with microtubules, centrosome positioning, and cell polarity. *J. Cell Biol.* **191,** 585–598
33. Owen, D. J., Collins, B. M., and Evans, P. R. (2004) Adaptors for clathrin coats. Structure and function. *Annu. Rev. Cell Dev. Biol.* **20,** 153–191
34. Osterweil, E., Wells, D. G., and Mooseker, M. S. (2005) A role for myosin VI in postsynaptic structure and glutamate receptor endocytosis. *J. Cell Biol.* **168,** 329–338
35. Godreau, D., Vranckx, R., Maguy, A., Goyenvalle, C., and Hatem, S. N. (2003) Different isoforms of synapse-associated protein, SAP97, are expressed in the heart and have distinct effects on the voltage-gated K+ channel Kv1.5. *J. Biol. Chem.* **278,** 47046–47052
36. Maïga, O., Philippe, M., Kotelevets, L., Chastre, E., Benadda, S., Pidard, D., Vranckx, R., and Walch, L. (2011) Identification of mitogen-activated protein/extracellular signal-responsive kinase kinase 2 as a novel partner of the scaffolding protein human homolog of disc-large. *FEBS J.* **278,** 2655–2665
37. Montgomery, J. M., Zamorano, P. L., and Garner, C. C. (2004) MAGUKs in synapse assembly and function. An emerging view. *Cell Mol. Life Sci.* **61,** 911–929
38. Almeida, C. G., Yamada, A., Tenza, D., Louvard, D., Raposo, G., and Coudrier, E. (2011) Myosin 1b promotes the formation of post-Golgi carriers by regulating actin assembly and membrane remodelling at the trans-Golgi network. *Nat. Cell Biol.* **13,** 779–789
39. Carreno, S., Engqvist-Goldstein, A. E., Zhang, C. X., McDonald, K. L., and Drubin, D. G. (2004) Actin dynamics coupled to clathrin-coated vesicle formation at the trans-Golgi network. *J. Cell Biol.* **165,** 781–788
40. Motley, A., Bright, N. A., Seaman, M. N., and Robinson, M. S. (2003) Clathrin-mediated endocytosis in AP-2-depleted cells. *J. Cell Biol.* **162,** 909–918
41. Warner, C. L., Stewart, A., Luzio, J. P., Steel, K. P., Libby, R. T., Kendrick-Jones, J., and Buss, F. (2003) Loss of myosin VI reduces secretion and the size of the Golgi in fibroblasts from Snell's waltzer mice. *EMBO J.* **22,** 569–579
42. Michaux, G., Dyer, C. E., Nightingale, T. D., Gallaud, E., Nurrish, S., and Cutler, D. F. (2011) A role for Rab10 in von Willebrand factor release discovered by an AP-1 interactor screen in *C. elegans*. *J. Thromb. Haemost.* **9,** 392–401
43. Michaux, G., and Cutler, D. F. (2004) How to roll an endothelial cigar. The biogenesis of Weibel-Palade bodies. *Traffic* **5,** 69–78
44. Gardoni, F., Mauceri, D., Marcello, E., Sala, C., Di Luca, M., and Jeromin, A. (2007) SAP97 directs the localization of Kv4.2 to spines in hippocampal neurons. Regulation by CaMKII. J. Biol. *Chem.* **282,** 28691–28699
45. Sans, N., Racca, C., Petralia, R. S., Wang, Y. X., McCallum, J., and Wenthold, R. J. (2001) Synapse-associated protein 97 selectively associates with a subset of AMPA receptors early in their biosynthetic pathway. *J. Neurosci.* **21,** 7506–7516
46. Nash, J. E., Appleby, V. J., Corrêa, S. A., Wu, H., Fitzjohn, S. M., Garner, C. C., Collingridge, G. L., and Molnár, E. (2010) Disruption of the interaction between myosin VI and SAP97 is associated with a reduction in the number of AMPARs at hippocampal synapses. *J. Neurochem.* **112,** 677–690